ACS Chemical Neuroscience

pubs.acs.org/chemneuro

Research Article

Partitioning of Catechol Derivatives in Lipid Membranes: Implications for Substrate Specificity to Catechol-*O*-methyltransferase

Petteri Parkkila* and Tapani Viitala

Cite This: *ACS Chem. Neurosci.* 2020, 11, 969–978

Read Online

ACCESS | Metrics & More | Article Recommendations | Supporting Information

ABSTRACT: We have utilized multiparametric surface plasmon resonance and impendance-based quartz crystal microbalance instruments to study the distribution coefficients of catechol derivatives in cell model membranes. Our findings verify that the octanol–water partitioning coefficient is a poor descriptor of the total lipid affinity for small molecules which show limited lipophilicity in the octanol–water system. Notably, 3-methoxytyramine, the methylated derivative of the neurotransmitter dopamine, showed substantial affinity to the lipids despite its nonlipophilic nature predicted by octanol–water partitioning. The average ratio of distribution coefficients between 3-methoxytyramine and dopamine was 8.0. We also found that the interactions between the catechols and the membranes modeling the cell membrane outer leaflet are very weak, suggesting a mechanism other than the membrane-mediated mechanism of action for the neurotransmitters at the postsynaptic site. The average distribution coefficient for these membranes was one-third of the average value for pure phosphatidylcholine membranes, calculated using all compounds. In the context of our previous work, we further theorize that membrane-bound enzymes can utilize membrane headgroup partitioning to find their substrates. This could explain the differences in enzyme affinity between soluble and membrane-bound isoforms of catechol-*O*-methyltransferase, an essential enzyme in catechol metabolism.

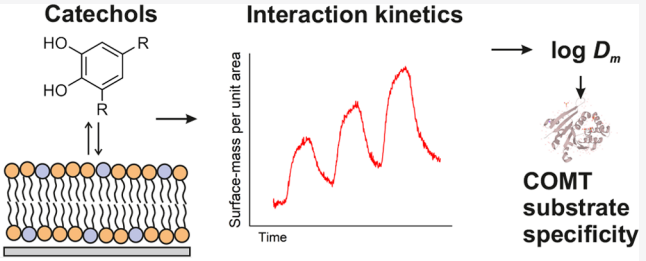

KEYWORDS: *Catechols, partition coefficient, distribution coefficient, supported lipid bilayer, multiparametric surface plasmon resonance, quartz crystal microbalance*

INTRODUCTION

Octanol–water partition coefficient for an un-ionized compound (log $P_{oct/w}$) is a descriptor for the ability of small molecular drugs to passively permeate through the cellular membranes of the body.[1,2] It belongs to the Lipinski's rule of five parameters which describe the drug-likeness of a molecule.[3] Ghose et al. have later suggested a qualifying range of −0.4 to 5.6 for log $P_{oct/w}$, and since then the importance of pH-dependent dissociation in the prediction of drug behavior in the body compartments has been acknowledged.[4,5] While the pH-dependent counterpart of the partition coefficient, distribution coefficient (log $D_{oct/w}$), should be used instead of log $P_{oct/w}$ for studying compounds, the correlation between log $P_{oct/w}$ or log $D_{oct/w}$ and lipid membrane partitioning is sometimes assumed.[6] However, electrostatic interactions and the capability for compounds to form hydrogen bonds with the lipid headgroups at the membrane-water interface are not taken into account by the octanol–water partitioning coefficients.[7] In a more rigorous treatment of the analyte binding, two partition coefficients should be described, one for the aqueous-interfacial binding and another for the partitioning from the interface to the bilayer interior.[8,9] Interfacial partitioning of charged or polar compounds may aid the passage of the molecules indirectly by allowing associated transport proteins to find them via lateral diffusion.[10] On the other hand, both integral and peripheral proteins operating as enzymes or signal transductors may require that the substrates reside at the lipid–water interface.[11,12] In the complex biological environment, molecules are affected not only by the local ion distribution, the pH, and the charge at the membrane–water interface, but also by the neighboring proteins that may be glycosylated. The local pH at the lipid–water interface can be strongly modulated by the net charge of the lipid headgroups, thus affecting the relative amounts of charged and neutral species of compounds in the interface.[8,13]

During recent years, membrane interactions of dopamine, an important neurotransmitter, have gained increasing inter-

Received: January 29, 2020
Accepted: February 26, 2020
Published: February 26, 2020

https://dx.doi.org/10.1021/acschemneuro.0c00049
ACS Chem. Neurosci. 2020, 11, 969–978

est.[14−17] In physiological pH, dopamine is mostly positively charged, interacting dominantly with the negatively charged phospholipids.[15] Molecular dynamics simulations have suggested that calcium can prevent dopamine aggregation to the inner leaflet of presynaptic vesicles.[17] Postila et al. have highlighted the selective role of the cell membrane on synaptic neurotransmission.[10] These results are plausible since nearly four decades ago Ohki found that cationic forms of local anesthetics adsorbed on negatively charged membranes, and calcium was capable of inhibiting this accumulation, at least at low concentrations.[18] Later, Barthel et al. expanded the model of the simple linear relation between the membrane-bound and free drug to account for surface saturation.[19] While it is believed that dopamine is not capable of crossing the membrane passively, Matam et al. found evidence on passive leakage of dopamine from the interior of closed lipid vesicle.[16] Overall, interactions of dopamine with the lipid membrane are complex, highlighting the importance of further studies on catechol compounds interacting with lipid membranes.

We have recently suggested that the membrane-bound isoform of catechol-*O*-methyltransferase (MB-COMT) is an interfacial enzyme.[12] The methylating hydroxy group in the 3-*O* position of the catechol ring has been found to orient outward from the lipid membrane,[14,16] while binding of the *S*-adenosyl-L-methionine cofactor brings the soluble part of the enzyme closer to the water−membrane interface. After the catalytic cycle performed by MB-COMT in the endoplasmic reticulum of postsynaptic nerve cells, a methylation product is formed, which in turn can be metabolized. In the case of dopamine, its methylation product 3-methoxytyramine (3-MT) is transformed into homovanillic acid (HVA) by the monoamine oxidase (MAO) enzyme located in the outer leaflet of the mitochondrial membrane. Surprisingly little is known about the interaction of 3-MT with the membranes despite its importance in dopamine metabolism. From a purely physicochemical point-of-view, the addition of a methyl group in the 3-*O* position of the catechol group should increase the lipophilicity of the molecule. Indeed, the reported log $P_{oct/w}$ of 3-MT is −0.08, making it ∼250 times more lipophilic than dopamine with a log $P_{oct/w}$ of −2.38 when the molecules are uncharged.[20] At physiological pH, however, both of these molecules become positively charged with experimental distribution coefficients (log $D_{oct/w}$) of −2.22 and −2.48, respectively, showing negligible lipophilicity. Another interesting catechol derivative is the precursor form of dopamine and an anti-Parkinson agent, L-dopa (levodopa), which as a zwitterionic amino acid is considered nonpolar overall, but carries both positive and negative charge at physiological pH. Based on the previous study using molecular dynamics simulations, these charged groups of L-dopa are capable of forming hydrogen bonds with the lipid headgroups.[14] However, the strength of the partitioning was not studied experimentally apart from a simple qualitative study using Langmuir monolayers.[14]

The size of fluorescent probes is usually comparable to the size of the compounds of interest, and utilizing properties other than the intrinsic fluorescence of the compounds when studying membrane interactions is questionable. Unfortunately, label-free techniques capable of resolving the full membrane-binding characteristics, namely, the location and orientation of small molecules in the membrane, are scarce. Nuclear magnetic resonance remains as the most powerful technique for this purpose but requires extensive preparations and expertise.[21] Other techniques such as isothermal titration calorimetry suffer from low throughput but allow the separation of entropic and enthalpic components of the binding process. However, label-free methods measuring physical changes occurring in the vicinity of a solid surface have high time-resolving properties, and real-time measurements of binding of an analyte on a lipid bilayer are possible. As a downside, spatial resolution and sensitivity for nonspecific binding are somewhat limited. In the surface plasmon resonance technique (SPR), the spatial limit is characterized by the decay length of the *p*-polarized electric field perpendicular to the sensor surface. Throughput is superior to other label-free techniques, and allows multiple parallel measurements. Another popular label-free technique, quartz crystal microbalance (QCM), employs measurement of the changes of the oscillation frequency of a quartz crystal resonator upon a mass change on the surface. In QCM, the limiting distance above the surface is the decay length of the shear-wave in the measurement cell.

In the present study, membrane partitioning of five different catechol derivatives is studied (Figure 1). The partitioning was

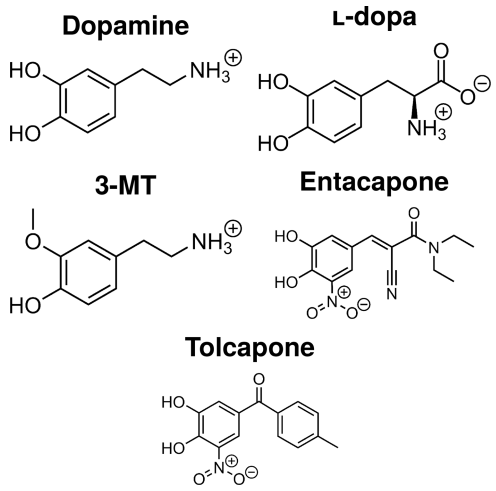

Figure 1. Chemical structures of the studied catechol derivative compounds. Formal charges are indicated at pH = 7.4. The nitrite group in tolcapone and entacapone has a net negative charge.

investigated using the label-free surface-sensitive methodologies, multiparametric surface plasmon resonance, and quartz crystal microbalance. In addition to dopamine, L-dopa, and 3-MT, two prominent anti-Parkinson drugs, tolcapone and entacapone, were chosen due to their well-known physicochemical properties and their different affinities toward the soluble and membrane-bound isoforms of catechol-*O*-methyltransferase.[12,22] Both of the anti-Parkinson drugs can cause mitochondrial dysfunction, and they have shown dose-dependent hepatotoxicity in clinical trials.[23] Four supported lipid bilayer (SLB) compositions are employed as cell membrane biomimetic platforms: zwitterionic, electrically neutral DOPC (PC, later in the paper); anionic, negatively charged DOPC−DOPS in the molar ratio of 8:2 (PC-PS); inner leaflet or endoplasmic reticulum model membrane consisting of DOPC−DOPE−DOPS in the molar ratio of 11:15:6 (PC-PE-PS), and extracellular leaflet membrane model consisting of DOPC−sphingomyelin−cholesterol in an equimolar mixture (PC-Sm-Chol). We have used a simple kinetic titration setup to measure analyte binding to the lipid

https://dx.doi.org/10.1021/acschemneuro.0c00049
ACS Chem. Neurosci. 2020, 11, 969−978

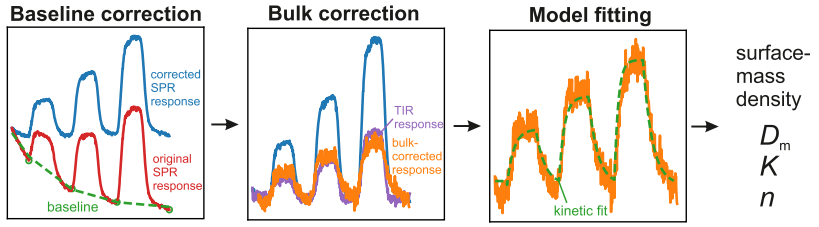

Figure 2. Depiction of the analysis process performed on the surface plasmon resonance data for the extraction of the binding parameters.

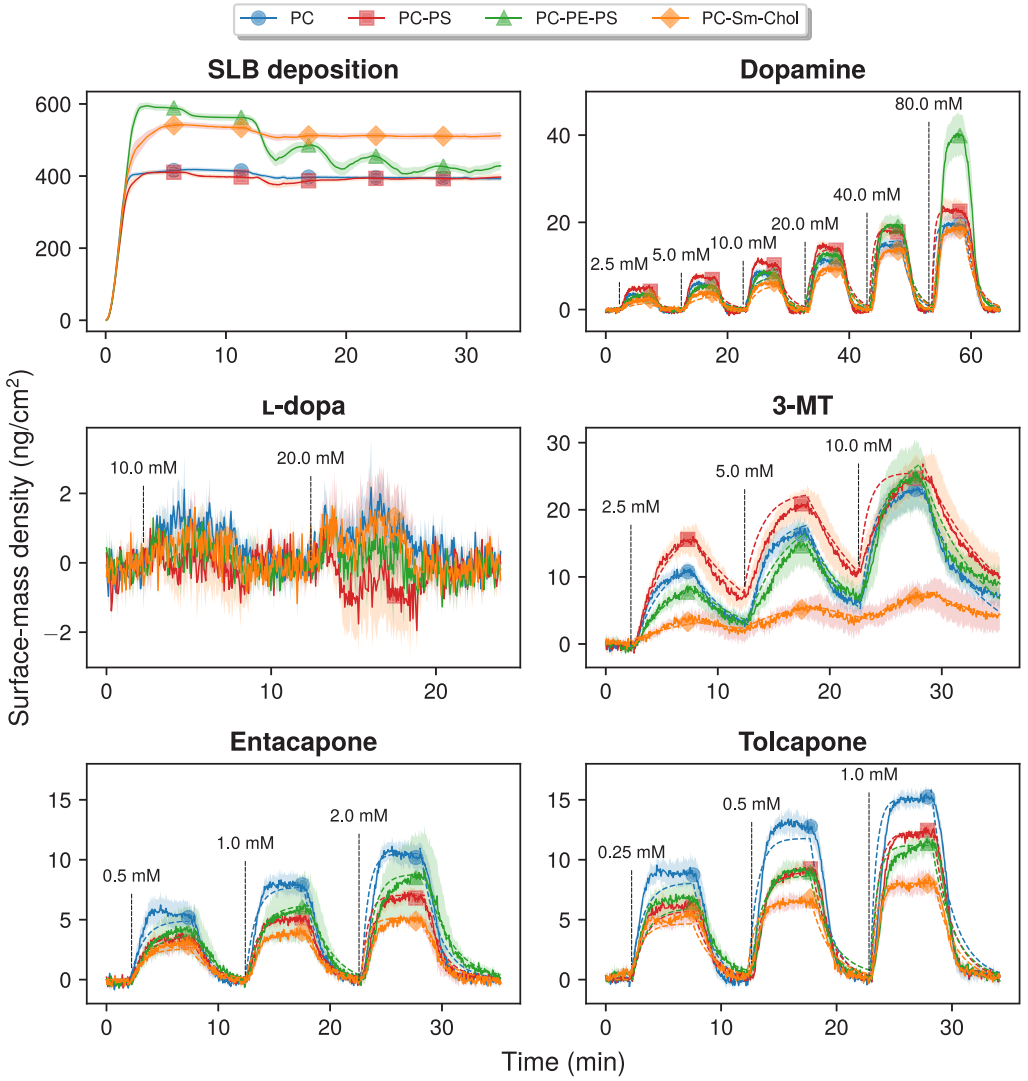

Figure 3. Average surface-mass densities as a function of time for the deposition of SLBs and different catechol compounds ($N = 4$). Dashed lines show the kinetic fits using the one-site kinetic model, and shaded areas represent the standard error of the mean.

membranes. In principle, this allows one to derive all relevant interaction parameters in a single experiment: log D_m, logarithm of the membrane distribution coefficient (K_m or K_p by some authors); n, number of available lipid-binding sites for an analyte, and K, mole ratio distribution coefficient. In addition, the multiparametric surface plasmon resonance instrument can simultaneously be used as a refractometer to derive refractive index increments (dn/dC) of the analytes (eq S14) and exploited to account for bulk contribution to the SPR response from the high concentrations of analytes (eq S13). Characterization of the supported lipid membranes (thickness, refractive index, surface-mass density) has been performed in our previous work.[24]

RESULTS

Surface Plasmon Resonance Kinetic Measurements. The conventional surface plasmon resonance technique records the change in the SPR peak minimum angle, referred to as the "SPR response". In multiparametric SPR, since the whole SPR reflectance curve is obtained, the angle of total internal reflection (TIR) can be used to subtract the optical contribution from the varying bulk concentration of an analyte. After the bulk correction, the SPR response can be converted

https://dx.doi.org/10.1021/acschemneuro.0c00049
ACS Chem. Neurosci. 2020, 11, 969−978

Table 1. Results from the Modeling of the Surface Plasmon Resonance Binding Data

		kinetic model				linear model		
		D_m	log D_m	n	K (M^{-1})	D_m	log D_m	log $D^{ref}_{oct/w}$
dopamine	PC	18	1.26	0.66	41	19	1.28	−2.48[20]
	PC-PS	24	1.37	0.74	48	25	1.40	
	PC-PE-PS	16	1.21	0.96	23	18	1.25	
	PC-Sm-Chol	10	1.00	0.45	25	10	1.02	
L-dopa	PC					1.4	0.14	−2.39[20]
	PC-PS					0.2	−0.82	
	PC-PE-PS					0.6	−0.20	
	PC-Sm-Chol					0.5	−0.27	
3-MT	PC	152	2.18	0.76	304	53	1.72	−2.22[20]
	PC-PS	339	2.53	0.73	704	67	1.83	
	PC-PE-PS	97	1.99	1.21	110	47	1.67	
	PC-Sm-Chol	34	1.53	0.16	243	13	1.12	
entacapone	PC	68	1.83	0.22	471	69	1.84	0.18[25]
	PC-PS	38	1.58	0.15	384	44	1.65	
	PC-PE-PS	52	1.72	0.18	406	51	1.71	
	PC-Sm-Chol	28	1.45	0.06	526	29	1.46	
tolcapone	PC	572	2.76	0.31	2754	244	2.39	1.03[25]
	PC-PS	325	2.51	0.29	1712	174	2.24	
	PC-PE-PS	343	2.54	0.21	2267	165	2.22	
	PC-Sm-Chol	253	2.40	0.09	3030	100	2.00	

Table 2. Results from the Modeling of the Quartz Crystal Microbalance Binding Data[a]

		Γ_{QCM}	Γ_{SPR}	$\Delta f_{3,N}$ (Hz)	$\Delta f^{bulk}_{3,N}$	ΔD_3 (10^{-6})	ΔD^{bulk}_3
dopamine	PC	18.0	19.3	−9.3	−8.3	3.3	3.1
	PC-PS	111.0	22.6	−10.1		4.2	
	PC-PE-PS	174.8	40.3	−22.0		6.3	
	PC-Sm-Chol	35.8	18.6	−10.8		3.4	
3-MT	PC	145.3	22.8	−5.6	−1.7	1.6	0.6
	PC-PS	172.7	25.4	−7.0		2.6	
	PC-PE-PS	755.8	25.4	−27.0		8.6	
	PC-Sm-Chol	212.8	6.8	−7.2		2.4	
entacapone	PC	90.2	10.5	−0.7	−0.5	0.3	0.1
	PC-PS	<0	7.0	−0.3		0.4	
	PC-PE-PS	36.0	8.7	−1.4		0.6	
	PC-Sm-Chol	13.7	5.1	−0.7		0.8	
tolcapone	PC	86.8	15.1	−1.3	−0.3	0.7	0.0
	PC-PS	22.7	12.3	−0.8		0.1	
	PC-PE-PS	250.7	11.2	−2.7		2.1	
	PC-Sm-Chol	6.7	8.0	−0.7		0.3	

[a]Γ_{SPR} is the surface-mass density (in ng/cm^2) calculated for the highest used concentration in SPR experiments for each compound (dopamine, 80 mM; 3-MT, 10 mM; entacapone, 2.0 mM; tolcapone, 1.0 mM). Γ_{QCM} is the corresponding surface-mass density calculated using the QCM technique, and $\Delta f_{3,N}$ and ΔD_3 indicate the changes in the normalized 3rd overtone frequency and energy dissipation, respectively. Superscript "bulk" denotes the change in the frequency and dissipation measured without SLBs.

to the surface-mass density, i.e., the bound mass per unit area of an analyte interacting with the lipid bilayer. Figure 2 presents our analysis process that was used for the surface plasmon resonance data. Figure 3 shows the variation of the bound surface-mass density as a function of time. For one ligand−analyte pair, SPR can be assumed to operate under pseudo-first-order kinetics where the concentration of lipids in the bilayer is not changing. The use of the traditional Langmuir model leads to the distribution coefficient and the ratio of concentrations of bound and free analyte, which is a dimensionless quantity. The distribution coefficient is proportional to the surface-mass density of the analyte at saturation and the mole ratio distribution coefficient, K (kinetic model, eq S8). To find these parameters, a one-site kinetic binding model was fitted to the kinetic titration data of Figure 3. Using the obtained value for the saturation surface-mass density, the number of available lipid-binding sites, n, can be calculated. However, if the equilibrium saturation concentration cannot be determined from the data due to the limitations in the compound solubility, for example, the calculation of the distribution coefficient should be made in the linear range of analyte binding (linear model, eq S9). Then, the distribution coefficient is proportional to the ratio of the bound surface mass of the analyte and the analyte concentration injected in the SPR flow channel. However, in this case, the number of available binding sites, n, cannot be obtained.

The distribution coefficients calculated from the data in Figure 3 along with the fitted parameters for the kinetic and

https://dx.doi.org/10.1021/acschemneuro.0c00049
ACS Chem. Neurosci. 2020, 11, 969−978

linear modeling are presented in Table 1. As expected, electrostatics play a role in how the different catechol compounds interact with the membrane. When compared to neutral PC membrane, the positively charged dopamine and 3-MT interact more strongly with the PC-PS membrane, with ratios in distribution coefficients (D_m) of 1.3 and 2.2 (PC-PS:PC), respectively. The presence of PE diminished this preference toward the PC-PS membrane, at least with the lower concentrations. Tolcapone and entacapone, carrying a net negative charge, preferred the neutral PC membrane (PC-PS:PC D_m ratios of 0.6). For the zwitterionic L-dopa, partitioning was weak overall regardless of the membrane composition (D_m = 0.2−1.4). The slightly negative mass obtained for L-dopa with the PC-PS membrane in Figure 3 can be attributed to the sensitivity of minimal peak angle minimum shifts for the bulk effect correction. When the membrane distribution coefficients are compared to the octanol−water distribution coefficients at pH = 7.4, it is evident that all the studied compounds interact with the membrane despite their low distribution coefficients. The ratio of D_m and $D_{oct/w}$ shows that this difference is 100-fold at minimum. Comparison of the two SPR analysis methods (kinetic model versus linear model) shows that there is a difference between the models for tolcapone and 3-MT. Thus, interactions of tolcapone and 3-MT with the membranes may not be best described by these simple models, or the bulk concentrations used in the titration are not adequate to reach saturation of the lipid-analyte interaction.

Quartz Crystal Microbalance Measurements. In Table 2, surface-mass densities obtained from the viscoelastic modeling of the QCM data are compared to their SPR counterparts. The QCM time traces of the surface-mass densities for SLB formation and analyte binding are presented in Figures S6 and S7. Mass values determined using SPR and QCM are not expected to match due to the changes in sensor-coupled water, which leads to a higher measured mass in QCM. However, for the PC lipid bilayer, surface-mass densities agree quantitatively at the highest bulk concentration of dopamine (80 mM): 19 ng/cm^2 in SPR and 18 ng/cm^2 in QCM. A simple model where dopamine molecules are considered as spherical particles with a molar volume of 123 cm^3/mol gives an estimated saturation mass of 15 ng/cm^2 for a monolayer of dopamine on the surface of the bilayer.[26] In contrast to other catechol derivatives, 3-MT has a high average difference between the energy dissipation values obtained with the SLBs and the plain quartz crystal (3.2×10^{-6}, Table 2 and Figure S7). Therefore, prominent changes in the viscoelastic properties of the membrane induced by 3-MT are likely indicating that interactions of 3-MT with the membrane cannot be attributed only to the interfacial binding, and hydration detected by the QCM technique. In agreement with the SPR data, surface-mass densities calculated for the interaction with the PC-Sm-Chol bilayer are lower than for the other membrane compositions.

Quantitative Structure−Activity Relationship Modeling of the Membrane Partitioning. To study the ability to model the membrane distribution coefficients from the predicted structural data (number of hydrogen bond acceptors and donors; physiological charge; polar surface area), we investigated 12 compounds studied by Osanai et al.[6] and the catechol compounds using the exploratory linear regression analysis (see the Supporting Information, eq S15). Figure 4 shows that, for lipophilic compounds (log $P_{oct/w}$ > 2),

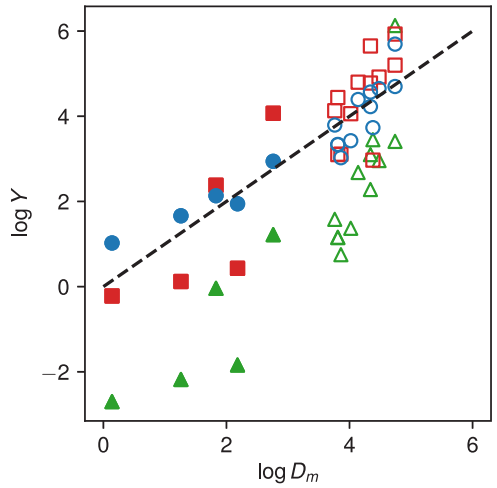

Figure 4. Logarithm of the membrane partition cofficient (log D_m) plotted against log Y where $Y = D_{m,pred}$, the predicted membrane distribution coefficient calculated using the linear regression analysis (blue circles); $Y = P_{oct/w}$, the partition coefficient (red squares); and $Y = D_{oct/w}$, the distribution coefficient at pH = 7.4 (green triangles). Open markers represent the membrane partitioning data from Osanai et al.,[6] and closed markers correspond to the studied catechol derivatives. The dashed black line shows where the parameters in horizontal and vertical axes are equal.

membrane partitioning is slightly overestimated by log $P_{oct/w}$ and vastly underestimated by log $D_{oct/w}$. However, for the catechol compounds, both log $P_{oct/w}$ and log $D_{oct/w}$ fail to describe the overall strength of the membrane partitioning. The R^2 value for the entire data set when using the sum of hydrogen bond donors and acceptors (#HA + #HD) together with log $D_{oct/w}$ as features was 0.856. Using log $P_{oct/w}$ instead of log $D_{oct/w}$ resulted in only a slight decrease in R^2 for the all compounds (decrease from 0.856 to 0.800). Restricting the set of compounds to the five catechol compounds (Table 1, PC lipid bilayer) resulted in a decrease of R^2 from 0.717 to 0.509. The linear model was able to estimate log D_m of dopamine, 3-MT, entacapone, and tolcapone relatively well, with the ratio of predicted D_m and measured D_m in the range of 0.6−2.5 (Figure 4 and Table S2).

DISCUSSION

Our results for the neurotransmitter dopamine can be quantitatively compared to the earlier studies using biophysical experiments. Assuming the available concentration of lipids for binding in the isothermal titration calorimetry measurement cell is γc_l = 0.5 × 1.43 M = 0.715 M in the study of Jodko-Piorecka and Litwinienko (half of the lipids are available for binding), the distribution coefficient for neutral DMPC can be estimated to be 39 with the assumption of n = 0.66 in Table 1.[15] This agrees well with our value of 18 for DOPC given the differences in experimental conditions and the fact that they did not use a buffer with a physiological concentration of salt. At least a 2-fold reduction in the equilibrium mole ratio distribution coefficient K was observed by Ikonen et al. when salt concentration was decreased from 150 to 15 mM.[27] The estimated K in the study of Jodko-Piorecka and Litwinienko[15] was 82.3 M^{-1} for pure PC vesicles, which indicates 2-fold stronger affinity (K = 41.5 M^{-1} in Table 1). The comparison is important since lipid molecules in supported lipid membranes have been criticized to have lower mobility than free-standing

https://dx.doi.org/10.1021/acschemneuro.0c00049
ACS Chem. Neurosci. 2020, 11, 969−978

bilayers in vesicles, making permeation of compounds in the membrane more difficult.[28] In the case of compounds interacting mainly with the membrane surface, however, these differences are expected to be minimal. The combination of information from SPR and QCM experiments suggests that surface interactions are predominant for dopamine, but some degree of membrane insertion is possible at the higher concentrations of the analyte (>40 mM).

Supported lipid bilayer modeling the endoplasmic reticulum membrane (PC-PE-PS) showed distinct behavior when compared to other membranes, having the highest bound mass when 80 mM of dopamine was introduced. This can be partly due to the morphological defects in the membrane. Having high amounts of negative curvature-inducing PE in the vesicles makes it difficult to spread them as supported membranes, requiring multiple osmotic shocks using injections with pure water. Even then, somewhat high energy dissipation values for the final PE-containing bilayers ($\sim 5 \times 10^{-6}$) suggests that the formed bilayer is imperfect. This could also explain the higher fluctuations in the bound mass, seen as relatively high standard deviation for entacapone and 3-MT and generally high surface-mass densities using the QCM technique. However, given that the catechol derivatives did not show substantial affinity toward the PE membrane and the results of Matam et al.[16] which indicate that dopamine is capable of leaking through the membranes, it could be that the curvature-induced defects induced by the presence of PE can lead to intercalation of dopamine inside the membrane. On the other hand, sterical protection of the nitrogen atom of the choline moiety in a PC headgroup makes the positive charge of the nitrogen less available when compared to ethanolamine in a PE headgroup. Therefore, PE is more available for hydrogen bonding with the surrounding water and susceptible for charge repulsion between the nitrogen and positively charged amine in the dopamine and 3-MT molecules.

The experimental results agree fairly well with the studies for dopamine and L-dopa performed using molecular dynamics simulations. Logarithmic distribution coefficients for the neutral PC membrane obtained by Postila et al.,[10] 1.06 for dopamine and 0.20 for L-dopa, are in good agreement with our experimental results (1.26 for dopamine and 0.14 for L-dopa). However, the calculated changes in free energy and distribution coefficients for the bilayers containing sphingomyelin and cholesterol or negatively charged PS have been very high in multiple studies, meaning that practically all analyte molecules are bound with lipids in simulations.[10,14,17] In our experiments, none of the analytes studied showed that drastic preference for the PC-Sm-Chol and PS-containing bilayers over the neutral PC, and for L-dopa there was no increase in membrane partitioning due to the hydrogen bonding suggested by the simulations. Also, the number of binding-sites (n) for the PC-Sm-Chol lipid bilayer is generally lower for all compounds (~0.19 on average). On average, distribution coefficients were three times higher for PC membranes when compared to PC-Sm-Chol membranes, calculated using all compounds. Since the amount of PC in the PC-Sm-Chol membranes is one-third of the amount in the pure PC membranes, this suggests that the studied molecules do not favorably partition to the dense and ordered domains formed by sphingomyelin and cholesterol, often called as lipid "rafts". We suspect the discrepancy between experiments and simulations is due to the small number of analyte molecules inside the simulation box, the overestimation of interactions with PS, Sm, and Chol in the force fields which are used in the simulations, and the absence of heterogeneities in the membranes. Proper scaling of the partial charges in lipid headgroups may be needed in order to get better correlation with the experimental results.

L-Dopa is known to be able to cross the blood-brain barrier (BBB) while the neurotransmitters dopamine and epinephrine cannot. Given the very low average distribution coefficient of L-dopa (~0.7), a passive transport mechanism across the BBB seems unlikely. Instead, as an amino acid precursor of dopamine, L-dopa is readily transported through the BBB by the L-type amino acid transporter LAT-1.[29] The results of very weak membrane binding of L-dopa regardless of the membrane type still do not exclude the membrane-mediated action of L-dopa as an antagonist of dopamine receptors as discussed by Postila et al.,[10] but subsequent experimental studies would be needed to confirm that hypothesis. In the quantitative structure−activity relationship modeling, the log D_m value of L-dopa, on the other hand, was overestimated, with a ratio of 7.9. Given the negative correlation of the sum of the predicted number of hydrogen bond acceptors and donors with the log D_m in the model, it is plausible that the low membrane distribution coefficient of L-dopa is due to the extensive hydrogen bonding between L-dopa and the water molecules, increasing the probability of L-dopa to reside in the water phase.

While the interactions of L-dopa with the membrane have been postulated to be surface-mediated, the dynamics of membrane interaction for the methylated form of dopamine, 3-MT, are not known. Interestingly, it was the only molecule in our study which showed clear irreversible binding to the lipid bilayer. The increase in the membrane distribution coefficient of 3-MT was nearly 10-fold when compared to dopamine, its nonmethylated counterpart, and the association and dissociation kinetics were slower, fitting better to the one-site kinetic model (Figure 3). The distribution coefficient for the outer leaflet model membrane (PC-Sm-Chol) was less than half of the corresponding coefficients for the other membranes. This is logical from a biological perspective since 3-MT is produced from dopamine by MB-COMT, located in the rough endoplasmic reticulum. Irreversible membrane binding of 3-MT and its capability to induce changes in the viscoelastic properties of the membrane, as shown by QCM experiments, differ drastically from to the qualities of its precursor dopamine lacking the methyl moiety from the 3-O position of the catechol ring. However, the average available sites for binding (n in Table 1) in the membrane are similar for both catechols ($n \approx 0.7$).

Inspection of the surface-mass densities for entacapone in SPR and QCM techniques (Table 2) suggests that entacapone as a bulky molecule has not prominent interaction with the bilayer interior. Indeed, molecular dynamics simulations have shown that entacapone tends to orient in the polar headgroup area perpendicular to the membrane normal in relation to the OCCO-group of the catechol ring.[12] In addition, entacapone induced negligible changes in the viscoelastic properties of the bilayers, indicated by the small changes in the energy dissipation. For tolcapone, changes in dissipation were somewhat higher, but it is not distinct whether this is due to the changes in interfacial water content, viscoelastic changes in the membrane, or both. For entacapone, surface-mass density for PC−PS composition was slightly negative, demonstrating the limitations in the sensitivity of the QCM instrument.

https://dx.doi.org/10.1021/acschemneuro.0c00049
ACS Chem. Neurosci. 2020, 11, 969−978

Therefore, QCM data should not be used as a quantitative tool for studying lipid−analyte interactions. Altogether, entacapone and tolcapone may interact mainly with the lipid−water interface, also supported by the moderate distribution coefficients of entacapone (0.18) and tolcapone (1.03), determined by Forsberg et al.[25] at pH 7.4. The obtained ratios of membrane distribution coefficient and octanol−water distribution coefficients are therefore 87 for entacapone and 103 for tolcapone, meaning that these compounds can have a 100-fold higher preference toward the lipid−water interface.

One critique that can be assigned to our experimental conditions is the presence of calcium in the preparation of SLBs with negatively charged phospholipids. Without calcium, these SLBs do not form due to the electrostatic repulsion between the vesicles and negatively charged silicon dioxide surface. Even after flushing with calcium-free buffer, trace amounts of calcium may irreversibly remain on the membrane surface, increasing the surface potential of the membrane. If we compare the ratio of membrane distribution coefficients of dopamine between PC−PS and PC membranes, 1.29, to the ratio of mole ratio partition coefficients, 1.73, obtained by Jodko-Piorecka and Litwinienko without calcium (25% DMPG),[15] our ratio is indeed much smaller. However, if we first correct this ratio to correspond to the relative amount of DOPS (20%) in our experiments using the linear relationship between the molar percentage of PS and mole ratio partition coefficient, the ratio drops to 1.58. Again, they used 20 mM phosphate buffer in the isothermal titration calorimetry experiments, while we used HBS buffer with 150 mM sodium chloride. Also, Ohki found a decrease in the zeta potential of phosphatidylserine vesicles due to the presence of calcium when the cationic anesthetic concentration was over millimolar range.[18] This result was probably due to the increase in positive charge repulsions between calcium, polar anesthetics, and sodium ions. On the other hand, it has been suggested that calcium ions can act as bridges between the anionic phospholipids and neurotransmitters.[30] We tested the effect of introducing EDTA after the bilayer formation on the binding of dopamine with the PC−PS membrane (Supporting Information Figure S2), and there was no measurable difference in the SPR response. Taking all this into consideration, we do not see the use of calcium in the bilayer formation process affecting analyte−membrane interactions in our experiments.

The obtained distribution coefficients for dopamine and L-dopa support our view for the catalytic mechanism of the membrane-bound enzyme MB-COMT.[12] When the proper orientation of molecules in the membrane−water interface is not a limiting factor, i.e., the hydroxy groups of the catechol ring are oriented outward from the membrane, the strength of partitioning becomes essential. This can be demonstrated by considering the ratio of Michaelis−Menten constants for MB-COMT and its soluble isoform, S-COMT. For human COMT expressed in baculovirus-infected insect cells, the calculated ratios are 13.7 for dopamine and 2.3 for L-dopa.[22] On the other hand, the same ratio calculated for dopamine in human brain-derived COMT extracts was 84.[31] The higher ratio could be attributed to different affinities and orientations of dopamine between human and insect membranes. In the current study, we have obtained the average distribution coefficients of 17 for dopamine and 0.7 for L-dopa. Therefore, we believe the capability of the membrane interface to act as a 'concentrator' is the likely explanation for the differences in catechol substrate specificity between S-COMT versus MB-COMT, a property for which no explanation has yet been found. The same mechanism may play a crucial role in interfacial catalysis performed by membrane proteins with similar structure and function. However, since the crystal structure of MB-COMT together with a catechol substrate is unavailable, this theory remains speculative. While the difficulty of obtaining structural data from any single-spanning transmembrane protein persists, indirectly derived theories are valuable in pointing to the direction where the subsequent studies should be headed.

In conclusion, membrane partitioning of several biologically or medicinally relevant catechol derivative compounds has been described using label-free surface-sensitive techniques. Comparison between octanol−water distribution coefficients and the obtained membrane distribution coefficients show that, for weakly or moderately lipophilic compounds having a combination of ionized and polar chemical groups, partitioning between the octanol and water phases does not correlate well with the overall strength of partitioning between lipid membrane and water. Four of the investigated compounds carry a net positive or negative charge in physiological pH, increasing their interactions with the charged moieties of the lipid headgroups. Dynamics of these interactions also include complex hydrogen bonding with both lipids and water molecules. The high number of hydrogen bonding atoms in L-dopa, for example, can lead to the low overall strength of partitioning to the membrane−water interface compared to other catechol derivatives. Dopamine and 3-MT showed a minor preference toward the negatively charged PC−PS membrane, while tolcapone and entacapone did not, owing to their negative net charge. While our experimental results were in quantitative agreement with the recent molecular dynamics studies performed on pure PC membranes, none of the studied compounds showed preferential affinity toward the outer leaflet membrane model, PC-Sm-Chol.[10,14,17] This leads us to believe that the interaction of neurotransmitters with sphingomyelin or the ordered sphingomyelin-cholesterol domains might have a limited role in the synaptic neurotransmission. 3-MT, a methylated metabolite of dopamine, showed substantial irreversible membrane affinity in contrast to dopamine and L-dopa. It is therefore plausible that, after the methylation cycle performed by the membrane-bound enzyme MB-COMT, 3-MT stays in the membrane and is capable of diffusing through the ER-Golgi contact network to be further processed by the monoamine oxidase enzyme. Intracellular membrane compartmentalization may then play an important role in the metabolite trafficking in postsynaptic neurons.

METHODS

Materials. 1,2-Dioleoyl-*sn*-glycero-3-phosphocholine (DOPC), 1,2-dioleoyl-*sn*-glycero-3-phosphoethanolamine (DOPE), egg sphingomyelin (Sm), and cholesterol (Chol) were obtained from Avanti Polar Lipids (Alabaster, AL), and 1,2-dioleoyl-*sn*-glycero-3-phospho-L-serine (DOPS) was obtained from Larodan AB (Solna, Sweden). 3,4-Dihydroxyphenethylamine hydrochloride (dopamine), 3,4-dihydroxy-L-phenylalanine (L-dopa, levodopa), 3-methoxy-4-hydroxyphenethylamine hydrochloride (3-methoxytyramine, 3-MT), 3,4-dihydroxy-4′-methyl-5-nitrobenzophenone (tolcapone), 2-cyano-*N*,*N*-diethyl-3-(3,4-dihydroxy-5-nitrophenyl)propenamide (entacapone), L-ascorbic acid, sodium chloride (NaCl), calcium chloride ($CaCl_2$), 4-(2-hydroxyethyl)-1-piperazineethanesulfonic acid (HEPES), chloroform ($CHCl_3$), 3-[(3-cholamidopropyl) dimethylammonio]-1-propanesulfonate (CHAPS), and ethylenediaminetetraacetic acid (EDTA) were from Sigma-Aldrich (St. Louis, MO). Ion-exchanged

https://dx.doi.org/10.1021/acschemneuro.0c00049
ACS Chem. Neurosci. 2020, 11, 969−978

ultrapure water (H_2O) with a resistivity of 18 MΩ cm from a Milli-Q purification system was used for the preparation of all solutions.

Sensor and Sample Preparation. Silica-coated SPR sensor slides and QCM crystals were obtained from BioNavis Ltd. (Tampere, Finland) and Q-Sense Inc./BiolinScientific (Västra Frölunda, Sweden), respectively. The washing procedures of the slides and crystals are described elsewhere.[24] All lipids were dissolved in chloroform stock solutions and mixed with the desired molar concentrations. Chloroform was first evaporated from the solution under a nitrogen stream, and thin-film hydration was performed at 50 °C temperature by first dispersing the lipids into an HBS-buffer (20 mM HEPES, 150 mM NaCl at pH 7.4) and then vigorously vortexing the suspension (1 mL, 5 mg/mL lipids). Vesicles were down-sized into small unilamellar vesicles using the bath sonication method (Elmasonic S 40 H, Elma Schmidbauer GmbH, Singen, Germany) at 50 °C with 10 min long cycles until the suspension was clear. Vesicles were stored at 4 °C until use. In order to aid the supported bilayer formation of the vesicles containing negatively charged DOPS, these vesicles were diluted prior to experiments in an HBS-buffer containing 5 mM $CaCl_2$. The lipid concentration in the experiments was always 0.15 mg/mL.

Experimental Procedures. A dual-wavelength multiparametric SPR (MP-SPR) instrument (SPR Navi 200, BioNavis Ltd., Tampere, Finland) was used together with a four-channel peristaltic pump system (Ismatec/Cole-Parmer GmbH, Wertheim, Germany). Different lipid compositions were used in each of the four channels during the four independent repeat measurements for each compound, resulting in a total of 80 data sets for analyte−lipid interactions. The impedance-based QCM Z-500 instrument (KSV Instruments Ltd., Helsinki, Finland) together with a two-channel peristaltic pump system (Ismatec/Cole-Parmer GmbH) was used for QCM experiments. One measurement was performed for each compound and lipid, resulting in a total of 20 data sets. Changes in frequency and dissipation were measured using the third, fifth, seventh, and ninth overtones.

Dopamine (stock solution of 200 mM), L-dopa (20 mM), and 3-MT (10 mM) were dissolved in HBS-buffer containing 2 mM of L-ascorbic acid (HBS+AA) to prevent oxidation. Solutions of entacapone (4.0 mM) and tolcapone (2.0 mM) were prepared in HBS-buffer containing 5% (v/v) DMSO (HBS+DMSO) to enhance solubility. The bulk concentrations of different compounds in the titration experiments were as follows: dopamine, 2.5, 5.0, 10, 20, 40, and 80 mM; L-dopa, 10 and 20 mM; 3-MT, 2.5, 5.0, and 10 mM; entacapone, 0.5, 1.0, and 2.0 mM in SPR, and 1.0, 2.0, and 4.0 mM in QCM; tolcapone, 0.25, 0.50, and 1.0 mM. L-dopa showed no measurable frequency shifts in QCM after the effect of the bulk signal was taken into account (data not shown).

SLB formation was performed by the injection of vesicle solution at the flow speed of 186 (SPR) or 250 (QCM) μL/min over the sensor surface. After a stabilization period by running vesicle-free HBS through the flow channels, the osmotic shock was induced using one or two ultrapure H_2O injections in order to ensure homogeneity of the SLBs. For the lipid formulation containing PE, two to four additional injections of H_2O were used. For the binding studies with different compounds, flow speeds were reduced to 56 (SPR) and 75 (QCM) μL/min. Each compound at different concentrations, described above, were flown over the supported lipid membrane for 5 min, followed by a 5 min dissociation phase between each concentration addition. Due to the sensitivity of the SPR instrument for the changes in optical properties of the running buffer, the buffer for dopamine, L-dopa, and 3-MT was changed from HBS to HBS+AA after the SLB formation. Also, buffer for entacapone and tolcapone was changed from HBS to HBS+DMSO after the SLB formation. In QCM measurements for entacapone and tolcapone, HBS+DMSO was also used as a running buffer for SLB formation, and vesicles were also diluted in this buffer. This was not done in SPR experiments since the use of DMSO increased the chances of air accumulation inside the flow channel of the SPR instrument.

Data Analysis. Figure preparation and most of the data analysis was performed using in-house scripts written in Python (v 3.7) using relevant libraries. Baseline correction of the lipid-analyte binding responses was performed using the manually selected time-points from the beginning of each concentration addition. Time-averaged response values were calculated, and linearly interpolated data points were then subtracted from the original data sets. Average values were calculated using the 16 data points (corresponding to 1 min) before the data points which were manually determined to account for the noise in the data. For 3-MT, no baseline correction was used due to the irreversible binding of 3-MT to the supported membranes used in the study. Change in the SPR peak minimum angle and the angle of total internal reflection (TIR) were corrected separately. In the end, the contribution of the TIR to the SPR peak minimum angle was subtracted. Details of the analysis performed with the SPR data are presented in the Supporting Information, based on the work of Jung et al. and Figueira et al.[32,33]

For the QCM experiments, the changes in the overtone frequencies and dissipations were also measured for the plain quartz crystal without any SLBs. The data was modeled using a rigid film (Sauerbrey condition) together with a bulk liquid with a varying density and fixed viscosity. The resulted mass values of the rigid film (analyte bound to the surface) were practically zero, and the resulting changes in the bulk liquid density were used in the subsequent fitting of the analytes binding to the lipid bilayer, in order to correct for the bulk contribution. Analytes interacting with SLBs were modeled using viscoelastic (Kelvin−Voigt) modeling.[34] The bilayer and the analyte were considered to compose a single layer above the oscillating quartz crystal, and the surface-mass densities of the pure lipid layer were subtracted from the mass values obtained after the binding of the analyte.

Some manual modifications of the data were necessary, and they are explained in detail here: (1) Manual baseline correction for SLB deposition data was made due to the visible baseline drift during the experiments. Baseline correction was performed manually using Origin Pro software (v. 2018b, OriginLab Corp., Northampton, MA) using the spline interpolation method. (2) In the first experiment for tolcapone (instrument channel 2, PC−PS lipid composition), a sudden baseline shift in the data was manually corrected. (3) Few isolated spikes in the tolcapone data sets were removed. Data sets without the baseline and TIR corrections are presented in Supporting Information Figures S3−S7.

■ ASSOCIATED CONTENT

Supporting Information

The Supporting Information is available free of charge at https://pubs.acs.org/doi/10.1021/acschemneuro.0c00049.

> Equations for the calculations of the SPR binding data; calculation of the decay length parameters; calculation of the sensitivity parameters; details of the quantitative structure−activity relationship modeling; effect of calcium on the analyte binding; unprocessed surface plasmon resonance data; unprocessed quartz crystal microbalance data (PDF)

■ AUTHOR INFORMATION

Corresponding Author

Petteri Parkkila − *Drug Research Program, Division of Pharmaceutical Biosciences, Faculty of Pharmacy, University of Helsinki, 00014 Helsinki, Finland;* orcid.org/0000-0002-2717-0232; Phone: +358 50 465 5801; Email: petteri.parkkila@helsinki.fi

Author

Tapani Viitala − *Drug Research Program, Division of Pharmaceutical Biosciences, Faculty of Pharmacy and Division of Pharmaceutical Chemistry and Technology, University of*

https://dx.doi.org/10.1021/acschemneuro.0c00049
ACS Chem. Neurosci. 2020, 11, 969−978

Helsinki, 00014 Helsinki, Finland; orcid.org/0000-0001-9074-9450

Complete contact information is available at: https://pubs.acs.org/10.1021/acschemneuro.0c00049

Author Contributions

P.P and T.V. designed the research and prepared the final manuscript. P.P carried out all experiments, analyzed the data, and wrote the initial draft of the manuscript.

Funding

This work was funded by personal thesis grants for P.P. from The Finnish Cultural Foundation and Magnus Ehrnrooth Foundation.

Notes

The authors declare no competing financial interest.

■ ABBREVIATIONS

3-MT, 3-methoxytyramine; Chol, cholesterol; COMT, catechol-*O*-methyltransferase; HVA, homovanillic acid; L-dopa, levodopa; MAO, monoamine oxidase; MP-SPR, multiparametric surface plasmon resonance; PC, phosphatidylcholine; PE, phosphatidylethanolamine; PS, phosphatidylserine; QCM, quartz crystal microbalance; Sm, sphingomyelin; SLB, supported lipid bilayer

■ REFERENCES

(1) Mälkiä, A., Murtomäki, L., Urtti, A., and Kontturi, K. (2004) Drug permeation in biomembranes. *Eur. J. Pharm. Sci. 23*, 13−47.
(2) Bennion, B. J., Be, N. A., McNerney, M. W., Lao, V., Carlson, E. M., Valdez, C. A., Malfatti, M. A., Enright, H. A., Nguyen, T. H., Lightstone, F. C., and Carpenter, T. S. (2017) Predicting a Drug's Membrane Permeability: A Computational Model Validated with in Vitro Permeability Assay Data. *J. Phys. Chem. B 121*, 5228−5237.
(3) Lipinski, C. A., Lombardo, F., Dominy, B. W., and Feeney, P. J. (1997) Experimental and computational approaches to estimate solubility and permeability in drug discovery and development settings. *Adv. Drug Delivery Rev. 23*, 3−25.
(4) Ghose, A. K., Viswanadhan, V. N., and Wendoloski, J. J. (1999) A knowledge-based approach in designing combinatorial or medicinal chemistry libraries for drug discovery. 1. A qualitative and quantitative characterization of known drug databases. *J. Comb. Chem. 1*, 55−68.
(5) Bhal, S. K., Kassam, K., Peirson, I. G., and Pearl, G. M. (2007) The rule of five revisited: Applying log D in place of log P in drug-likeness filters. *Mol. Pharmaceutics 4*, 556−560.
(6) Osanai, H., Ikehara, T., Miyauchi, S., Shimono, K., Tamogami, J., Toshifumi, N., and Kamo, N. (2013) A study of the Interaction of drugs with liposomes with Isothermal titration calorimetry. *J. Biophys. Chem. 4*, 11−21.
(7) Vaes, W. H., Ramos, E. U., Verhaar, H. J., Cramer, C. J., and Hermens, J. L. (1998) Understanding and estimating membrane/water partition coefficients: Approaches to derive quantitative structure property relationships. *Chem. Res. Toxicol. 11*, 847−854.
(8) Freiría-Gándara, J., Losada-Barreiro, S., Paiva-Martins, F., and Bravo-Díaz, C. (2018) Differential Partitioning of Bioantioxidants in Edible Oil-Water and Octanol-Water Systems: Linear Free Energy Relationships. *J. Chem. Eng. Data 63*, 2999−3007.
(9) Raimúndez-Rodríguez, E. A., Losada-Barreiro, S., and Bravo-Díaz, C. (2019) Enhancing the fraction of antioxidants at the interfaces of oil-in-water emulsions: A kinetic and thermodynamic analysis of their partitioning. *J. Colloid Interface Sci. 555*, 224−233.
(10) Postila, P. A., Vattulainen, I., and Róg, T. (2016) Selective effect of cell membrane on synaptic neurotransmission. *Sci. Rep. 6*, 1−10.
(11) Bondar, A. N., and Keller, S. (2018) Lipid Membranes and Reactions at Lipid Interfaces: Theory, Experiments, and Applications. *J. Membr. Biol. 251*, 295−298.
(12) Magarkar, A., Parkkila, P., Viitala, T., Lajunen, T., Mobarak, E., Licari, G., Cramariuc, O., Vauthey, E., Róg, T., and Bunker, A. (2018) Membrane bound COMT isoform is an interfacial enzyme: general mechanism and new drug design paradigm. *Chem. Commun. 54*, 3440−3443.
(13) Kundu, A., Yamaguchi, S., and Tahara, T. (2014) Evaluation of pH at charged lipid/water interfaces by heterodyne-detected electronic sum frequency generation. *J. Phys. Chem. Lett. 5*, 762−766.
(14) Orłowski, A., Grzybek, M., Bunker, A., Pasenkiewicz-Gierula, M., Vattulainen, I., Männistö, P. T., and Rõg, T. (2012) Strong preferences of dopamine and l-dopa towards lipid head group: Importance of lipid composition and implication for neurotransmitter metabolism. *J. Neurochem. 122*, 681−690.
(15) Jodko-Piorecka, K., and Litwinienko, G. (2013) First experimental evidence of dopamine interactions with negatively charged model biomembranes. *ACS Chem. Neurosci. 4*, 1114−1122.
(16) Matam, Y., Ray, B. D., and Petrache, H. I. (2016) Direct affinity of dopamine to lipid membranes investigated by Nuclear Magnetic Resonance spectroscopy. *Neurosci. Lett. 618*, 104−109.
(17) Mokkila, S., Postila, P. A., Rissanen, S., Juhola, H., Vattulainen, I., and Róg, T. (2017) Calcium Assists Dopamine Release by Preventing Aggregation on the Inner Leaflet of Presynaptic Vesicles. *ACS Chem. Neurosci. 8*, 1242−1250.
(18) Ohki, S. (1984) Adsorption of local anesthetics on phospholipid membranes. *Biochim. Biophys. Acta, Biomembr. 777*, 56−66.
(19) Barthel, D., Zschoernig, O., Lange, K., Lenk, R., and Arnold, K. (1988) Interaction of electrically charged drug molecules with phospholipid membranes. *Biochim. Biophys. Acta, Biomembr. 945*, 361−366.
(20) Mack, F., and Bönisch, H. (1979) Dissociation constants and lipophilicity of catecholamines and related compounds. *Naunyn-Schmiedeberg's Arch. Pharmacol. 310*, 1−9.
(21) Watts, A. (2005) Solid-state NMR in drug design and discovery for membrane-embedded targets. *Nat. Rev. Drug Discovery 4*, 555−568.
(22) Lotta, T., Vidgren, J., Tilgmann, C., Ulmanen, I., Melén, K., Julkunen, I., and Taskinen, J. (1995) Kinetics of Human Soluble and Membrane-Bound Catechol O-Methyltransferase: A Revised Mechanism and Description of the Thermolabile Variant of the Enzyme. *Biochemistry 34*, 4202−4210.
(23) Longo, D. M., Yang, Y., Watkins, P. B., Howell, B. A., and Siler, S. Q. (2016) Elucidating differences in the hepatotoxic potential of tolcapone and entacapone with DILIsym®, a mechanistic model of drug-induced liver injury. *CPT: Pharmacometrics Syst. Pharmacol. 5*, 31−39.
(24) Parkkila, P., Elderdfi, M., Bunker, A., and Viitala, T. (2018) Biophysical Characterization of Supported Lipid Bilayers Using Parallel Dual-Wavelength Surface Plasmon Resonance and Quartz Crystal Microbalance Measurements. *Langmuir 34*, 8081−8091.
(25) Forsberg, M. M., Huotari, M., Savolainen, J., and Männistö, P. T. (2005) The role of physicochemical properties of entacapone and tolcapone on their efficacy during local intrastriatal administration. *Eur. J. Pharm. Sci. 24*, 503−511.
(26) *ChemSpider*, https://www.chemspider.com/Chemical-Structure.661.html (accessed 2019-08-27).
(27) Ikonen, M., Murtomäki, L., and Kontturi, K. (2010) Microcalorimetric and zeta potential study on binding of drugs on liposomes. *Colloids Surf., B 78*, 275−282.
(28) Kannisto, K., Murtomäki, L., and Viitala, T. (2011) An impedance QCM study on the partitioning of bioactive compounds in supported phospholipid bilayers. *Colloids Surf., B 86*, 298−304.
(29) del Amo, E. M., Urtti, A., and Yliperttula, M. (2008) Pharmacokinetic role of L-type amino acid transporters LAT1 and LAT2. *Eur. J. Pharm. Sci. 35*, 161−174.

(30) Pérez-Isidoro, R., and Ruiz-Suárez, J. C. (2016) Calcium and protons affect the interaction of neurotransmitters and anesthetics with anionic lipid membranes. *Biochim. Biophys. Acta, Biomembr. 1858*, 2215−2222.
(31) Jeffery, D. R., and Roth, J. A. (1984) Characterization of Membrane-Bound and Soluble Catechol-O-Methyltransferase from Human Frontal Cortex. *J. Neurochem. 42*, 826−832.
(32) Jung, L. S., Campbell, C. T., Chinowsky, T. M., Mar, M. N., and Yee, S. S. (1998) Quantitative Interpretation of the Response of Surface Plasmon Resonance Sensors to Adsorbed Films. *Langmuir 14*, 5636−5648.
(33) Figueira, T. N., Freire, J. M., Cunha-Santos, C., Heras, M., Gonçalves, J., Moscona, A., Porotto, M., Salomé Veiga, A., and Castanho, M. A. (2017) Quantitative analysis of molecular partition towards lipid membranes using surface plasmon resonance. *Sci. Rep. 7*, 1−10.
(34) Nalam, P. C., Daikhin, L., Espinosa-Marzal, R. M., Clasohm, J., Urbakh, M., and Spencer, N. D. (2013) Two-Fluid Model for the Interpretation of Quartz Crystal Microbalance Response: Tuning Properties of Polymer Brushes with Solvent Mixtures. *J. Phys. Chem. C 117*, 4533−4543.

https://dx.doi.org/10.1021/acschemneuro.0c00049
ACS Chem. Neurosci. 2020, 11, 969−978